

Photoinduced Local Heating in Silica Photonic Crystals for Fast and Reversible Switching

Francisco Gallego-Gómez,* Alvaro Blanco, and Cefe López

Three-dimensional photonic crystals (PCs) have attracted a great deal of interest as optical components for accurate control of light propagation in all the space directions. These materials are periodic dielectric structures exhibiting a pseudo photonic bandgap (PBG) along certain lattice directions, which prohibits the propagation of light of a specific energy range. In order to increase the PC functionalities, a tunable PBG under external stimulus is highly desirable, especially in a reversible and fast fashion, to envisage applications such as dynamic filters, optical memories, switches and sensors. Artificial opals, consisting of solid colloidal crystals of self-assembled spheres, are widely employed as inexpensive and versatile PCs.^[1] Thereby, the PBG properties (position, width and reflectance/transmittance) are determined by, on the one hand, the opal topology and, on the other hand, the refractive indices of the spheres and their surrounding (opal voids, filled in general with air). This offers a straightforward way to obtain tunable PCs by infiltrating or functionalizing the opal with active materials (liquid crystals, photochromic molecules, elastomers, hydrogels, etc.) that respond under optical, magnetoelectric, mechanical, thermal or chemical stimuli.^[2–8] These strategies rely on prior opal modification, being generally time-consuming and experimentally difficult, requiring certain environments or needing sophisticated means of excitation. Moreover, tuning is commonly slow and not fully reversible.

Recently, it has been shown that silica artificial opals possess a PBG controllable by simply heating on a hot plate.^[9,10] Submicrometer silica spheres easily form high-quality face-centered-cubic (fcc) structures displaying a Bragg peak (the lowest energy PBG) in the visible range.^[11] Given the hydrophilic character of silica, these opals inherently contain a substantial amount of molecular water (as much as 8 wt% in as-grown samples) physisorbed on the silanol groups at the spheres surface.^[12,13] This water is partially placed between the spheres forming necks, leading to a non-close-packed arrangement, so that the opal lattice parameter (d_{111}) directly depends on the amount of water.^[9] Thus, controlled desorption of this water upon moderate heating induces large effects in the opal photonic properties, mostly due to the shrinking of d_{111} in up to 5%. Complete removal of the physisorbed water (achieved at ≈ 120 °C) leads to a pronounced blue-shift of the Bragg peak position (λ_{Bragg}) of up to 25 nm. PBG changes are reversible upon cooling down to

room temperature (RT) by virtue of spontaneous opal rehydration (i.e., re-adsorption of water on the spheres surface from ambient moisture). These results prove the high PBG tunability of bare silica opals by simply controlled water adsorption/desorption. However, changes occurred on the scale of seconds because of the slow heating/cooling of the whole sample.

Here, we demonstrate that this property can be exerted to induce millisecond PBG switching by photoinduced local heating. Therefore, we were aiming to heat the opal locally by irradiating a small area with a focused light beam of appropriate wavelength. Bare silica opals exhibit significant absorption at some bands in the UV and IR regions but not in the visible region (Figure 1), which would demand irradiation by costly and less-available UV or IR light sources. In addition, some of these bands strongly overlap with modes related to physisorbed water molecules,^[14] so light absorption would strongly decrease during the photoinduced water desorption. In order to avoid these drawbacks, we chose dyeing the opal by infiltration with an absorbing molecule in the blue/green region. This was readily achieved by simple casting of a neat chromophore on the opal spheres (see Experimental Section). The chromophore was chosen to absorb far from the opal PBG and exhibit a negligible optical response (like photochromism or photoluminescence) under the irradiation conditions. The infiltrated opal clearly absorbed in the visible region (Figure 1), proportionally to the content of the deposited chromophore, so that the absorbance was easily adjustable by varying the concentration of the cast solution. The Bragg peak shifted to longer wavelengths as a result of the partial filling of the opal voids by chromophore molecules, providing a direct estimate of the load of deposited dye in the infiltrated opal.^[15] In our case, we selected a chromophore filling fraction of $\approx 25\%$ of the void volume.

This approach enabled the use of inexpensive blue/green lasers to induce heating efficiently. The opal was photoirradiated with a focused 488 nm continuous-wave (cw) Ar⁺ laser while measuring the opal reflectance spectrum in order to monitor the PBG changes in situ. Photoirradiation was unnoticed by the bare opal, while it significantly affected the dye-infiltrated opal spectrum in a reversible fashion (Figure 2a). Under light exposure, the Bragg peak shifted to shorter wavelengths (up to 12 nm) within a few milliseconds and rapidly shifted back to the original position spontaneously after turning the light off. Simultaneously, the bandgap width decreased (up to 4%) during irradiation, also reversibly. This constitutes a moderate but rapid, fully reversible (without external stimulus) and highly reproducible PBG change, allowing reliable high-rate optical switching (Figure 2b). Long-term experiments demonstrated a high fidelity over millions of cycles. Measurable switching ($|\Delta\lambda_{\text{Bragg}}| \approx 1$ nm) was achieved at rates as fast as 200 Hz while longer cycles allowed larger PBG blue-shift and full relaxation.

Dr. F. Gallego-Gómez, Dr. A. Blanco, Prof. C. López
Instituto de Ciencia de Materiales de Madrid
C/ Sor Juana Inés de la Cruz 3, 28049 Madrid, Spain
E-mail: francisco.gallego@icmm.csic.es



DOI: 10.1002/adma.201202828

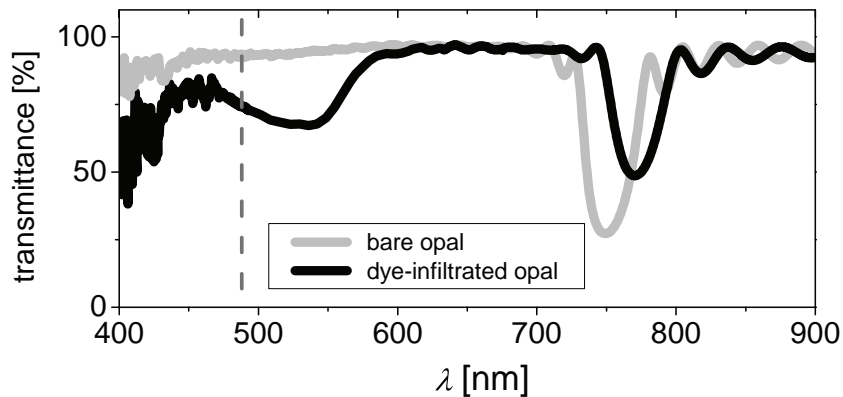


Figure 1. Transmission spectra of the bare silica opal (gray line) and after infiltration with the chromophore (black line). The dashed line indicates the excitation wavelength (488 nm from a cw Ar⁺ laser).

Figures 2c,d show the dynamics of both rise and decay of the spectral shift. The irradiation intensity determined the $\Delta\lambda_{\text{Bragg}}$ (Figure 3a), while it affected the dynamics only moderately (Figure 3b). Excitation above 40 W cm^{-2} led to significant dye photobleaching and a partially irreversible effect, and it was not included in the analysis.

The observed blue-shift is consistent with the expected water desorption due to opal heating under irradiation: the more pronounced, the higher the light intensity; while the reverse mechanism must be attributed to the opal rehydration upon cooling. The PBG changes measured at $I = 20 \text{ W cm}^{-2}$ (best performance)

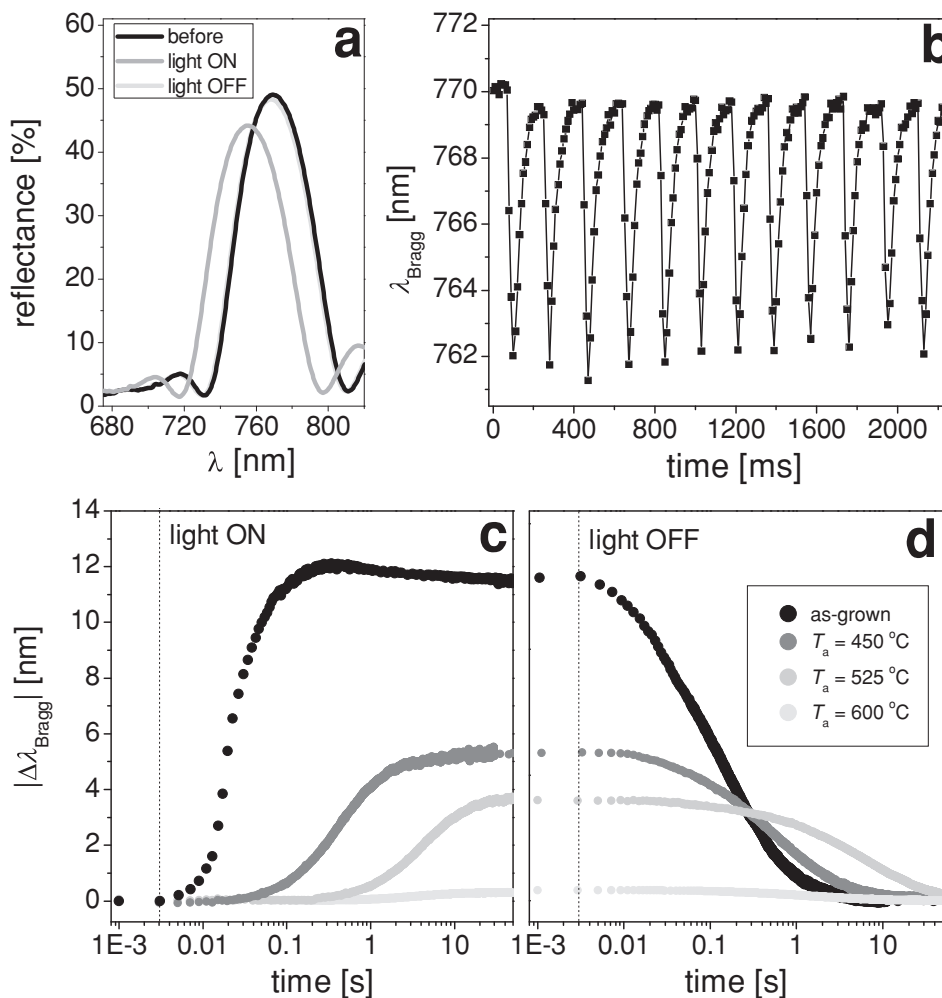


Figure 2. a) Bragg reflectance peak of a dye-infiltrated as-grown silica opal before, under photoirradiation (for 200 ms), and after relaxation (for 2 s). b) Modulation of λ_{Bragg} by photoswitching (laser on/off in 30/150 ms periods). Spectra were measured every 10 ms. c,d) Temporal evolution of $|\Delta\lambda_{\text{Bragg}}|$ in infiltrated as-grown (black symbols) and annealed (at 450, 525, and 600 °C (symbols with decreasing gray levels)) opals. The laser was turned on/off 2 ms after beginning the measurement (denoted by the dashed lines). In all cases, photoirradiation was performed on an area $S = 0.002 \text{ mm}^2$ and $I = 20 \text{ W cm}^{-2}$.

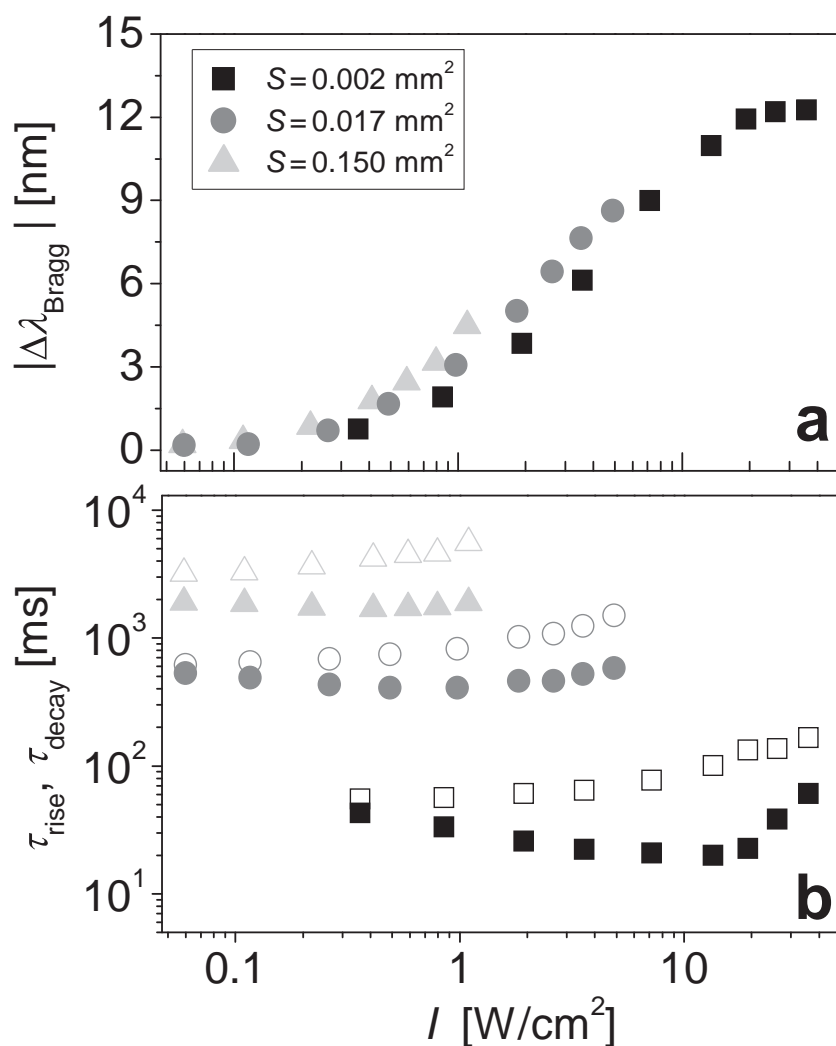


Figure 3. a) Intensity dependence of the stationary PBG blue-shift $|\Delta\lambda_{\text{Bragg}}|$. b) The rise and decay half-times τ_{rise} , τ_{decay} (solid and empty symbols, respectively) by irradiating three different irradiated areas S (0.002, 0.017 and 0.150 mm^2 : black, gray, and light gray symbols, respectively). All of the experiments were performed on infiltrated as-grown opals.

were analogous to those reported by Gallego-Gómez et al.^[9] by heating the whole opal at $\approx 50^\circ\text{C}$ due to the desorption of half the physisorbed water. Thereby, it was demonstrated that such changes (in particular, the narrowing of the bandgap) were mainly due to contraction of d_{111} (in $\approx 8 \text{ nm}$ (i.e., 2.5%)) as the water necks between the spheres diminished. On the contrary, the decrease of average refractive index in the opal voids (due to water removal) had a minor effect. Less effect is expected if the opal contains less adsorbed water. This was confirmed on silica opals subjected to thermal annealing (at temperature T_a), which progressively removed silanol groups from the silica surface^[16] so the opals became more hydrophobic.^[10,13] The PBG response in annealed opals (infiltrated with the same load of chromophore) gradually deteriorated with T_a (Figure 2c,d). On the one hand, the blue-shift notably declined, being negligible in the 600°C -annealed sample. The blue-shifts reasonably agreed with the values measured at 50°C on opals treated at similar T_a s.^[10] On the other hand, both shift induction and

posterior relaxation drastically slowed down, which indicates that both desorption and adsorption processes were hindered in the annealed opals compared to the as-grown one. This latter finding opens the possibility of studying dynamic sorption phenomena using this approach.

Obviously, the essential advantage of laser-induced opal heating is the fast heating rates, enabling pronounced water desorption in just a few milliseconds (unreachable by standard means). The spontaneous and rapid Bragg peak recovery after irradiation evidenced that heat was also rapidly dissipated through the opal structure (without active cooling), so water from the surrounding moisture could be quickly re-adsorbed. The localized photoabsorption of the focused laser enabled such efficiency of both thermal concentration – leading to fast heating – and posterior thermal dissipation – as the opal acts as thermal reservoir regarding the small hot spot. According to this statement, the extension of the irradiated area (S) must have strong influence on the performance dynamics (rather than on the stationary values). Indeed, this was verified by illuminating with different laser foci. The “steady-state” $|\Delta\lambda_{\text{Bragg}}|$, measured at the same I , increased only slightly with S (Figure 3a). As the irradiated volume became comparable with the total opal volume, the hot spot gradually affected the reservoir and a somewhat higher local temperature was attained. By contrast, the dynamics drastically slowed down with larger S and both the rise and decay half-times, τ_{rise} and τ_{decay} , increased from several milliseconds at $S = 0.002 \text{ mm}^2$ to seconds at $S = 0.150 \text{ mm}^2$ (Figure 3b). This indicates that heating/cooling of smaller opal volumes succeeded at faster rates. This also

suggests that the intrinsic limit of the dynamic range in this system has not been reached, but it is rather restricted by the smallest laser focus achievable in our setup.

Irrespective of the illuminated area, the local temperature rises with the intensity until reaching a maximum, which is given by the thermal equilibrium between the hot spot and the reservoir. This prevents higher heating of the spot and further water removal. This agrees with the increase of $|\Delta\lambda_{\text{Bragg}}|$ with I up to a maximum of $\approx 12 \text{ nm}$ (Figure 3a) although the maximum blue-shift reachable was approximately twice as much upon complete desorption.^[9] Regarding the dynamics, it slightly depended on I but exhibited recognizable features (Figure 3b). Upon irradiation, the PBG response accelerated (τ_{rise} decreased) with I , as expected since the absorption of more photons leads to faster heating. However, this enhancement saturated and the response slowed down by further increasing the intensity. A possible reason is that, beyond a certain threshold, the rapid warming of the surroundings limits the heating rate of the

irradiated spot. After switching the light off, the PBG recovery always became slower (τ_{decay} increased) with increasing I , as more heat needed to be dissipated. These features were more pronounced at smaller S , confirming the influence of the hot-spot size relative to that of the reservoir. Nevertheless, the system response with $S = 0.002 \text{ mm}^2$ was remarkably fast (with both buildup and decay times below 100 ms) over a larger range of intensities.

The kinetic features showed that both the desorption and re-adsorption processes essentially followed the heat dynamics of the irradiated spot, suggesting that fast water exchange at the silica surface occurred right after any change of the opal temperature. In particular, the water re-adsorption rates were comparable to the desorption ones (τ_{decay} was generally only 2- or 3-fold higher than τ_{rise}), probably facilitated by a high accessibility of the silica surface to the water vapor molecules through the large interstices between spheres. The photoexcitation of a restricted opal volume enabled fast temperature changes. In addition, as water desorption was limited to a reduced neighborhood, the surrounding moisture remained virtually unaltered and allowed fast restitution of the evacuated water in the opal. As capillary condensation is favored in a narrow space,^[17] the initial “refilling” of the necks between spheres may be easier. In any case, the water desorption and rehydration processes in the silica opal are expected to differ, in agreement with the hysteretic behavior observed upon conventional heating.^[9] It must be noted that the water affinity of the silica surface also played an important role in the dynamic processes as the performance clearly slowed down in the annealed (hydrophobic) opals (Figures 2c,d).

The energy dissipation through the opal can compromise the localization of the heat. This was investigated by illumination at a varying separations (x) from the point of the PBG measurement (Figure 4). By displacing the irradiation spot (increasing $|x|$), the photoinduced effect turned gradually inefficient as the PBG blue-shift deteriorated in both magnitude and response time, which proved the local character of the effect. This was most evident in the buildup dynamics, which slowed down two orders of magnitude by displacing the hot spot over 1 mm; such slowdown was less pronounced in the decay times. A remarkably large $|\Delta\lambda_{\text{Bragg}}|$ was still photoinduced even at distances of 1.5 mm. This confirms the partial heating beyond the irradiated spot, so the localization of the effect is smeared-out via thermalization of the whole structure. Moreover, this experiment allowed any nonthermal contributions of the chromophore to the effect to be discarded.

The features discussed so far are compatible with a thermally induced process leading to water desorption from the opal and subsequent PBG changes. To demonstrate such correspondence unambiguously, we simultaneously monitored, and compared both the change of water content and the PBG shift during the experiment. Therefore, the whole opal spectrum (UV-vis and IR range) was acquired in situ during and after laser irradiation, so that the amount of desorbed water ($\Delta(\text{H}_2\text{O})$) could be estimated from the decrease of the water-related IR absorption band at $\approx 2.9 \mu\text{m}$ (see Experimental). Figure 5a shows the evident loss of physisorbed water (increase of transmittance in the IR band) under light exposure, more pronounced in as-grown opals and gradually vanishing in annealed ones. Water was increasingly

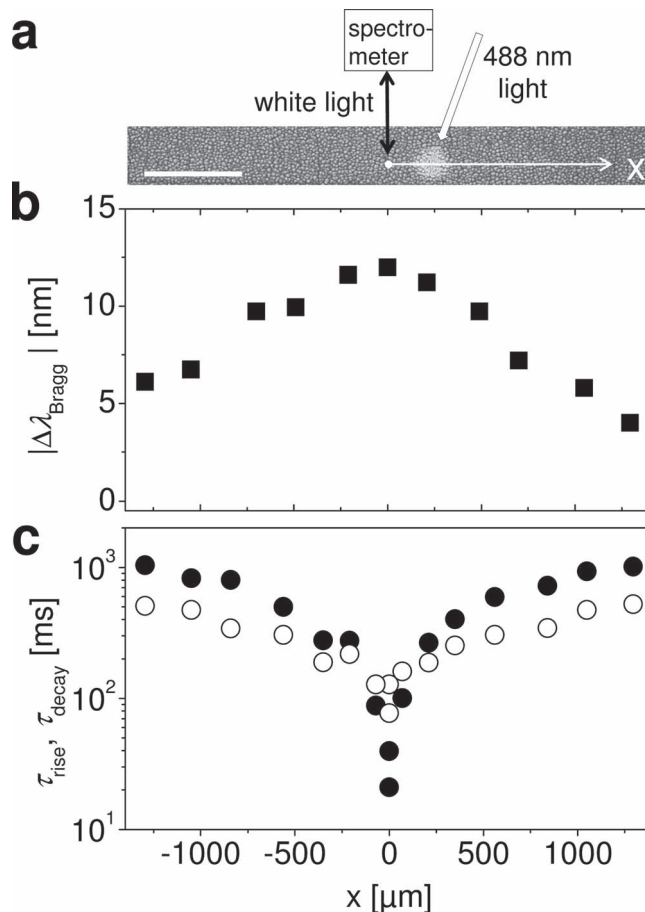


Figure 4. Local nature of the photoinduced PBG changes tested by displacing the irradiation spot from the measurement point a distance x . a) Optical microscopy image of the opal (with $\lambda_{\text{Bragg}} = 610 \text{ nm}$) under 488 nm laser excitation (lighter spot); the scale bar is 500 μm . A scheme of the setup and the defined x -axis are added. The white circle denotes the point at which the opal PBG was measured (area of $\approx 20 \mu\text{m}^2$). b) x dependence of $|\Delta\lambda_{\text{Bragg}}|$. c) x dependence of rise and decay half-times. Experiments were performed at $I = 20 \text{ mW cm}^{-2}$ and $S = 0.002 \text{ mm}^2$ in an infiltrated as-grown opal.

desorbed at higher laser intensity, reaching a maximum in the as-grown opal at about 30 W cm^{-2} (Figure 5b). The maximum corresponded to 45% of the maximum water content (that is, in the as-grown opal), in good agreement with the above discussed estimate of 50% from work by Gallego-Gómez et al.^[9] The IR-band absorbance was fully recovered after turning the laser off regardless of the intensity used in this range (Figure 5b), indicating that the removed water was completely re-adsorbed in all cases. These features resembled the behavior of the PBG shift. Indeed, by plotting the measured $\Delta\lambda_{\text{Bragg}}$ data (in different opals and at varying intensities) with the corresponding $\Delta(\text{H}_2\text{O})$ values, their correlation is evident (Figure 5c).

This correspondence holds for additional adsorption/desorption experiments using other means than photoabsorption. Thus, directing a flow of compressed-air or gas onto the bare opal also induced reversible water desorption and subsequent PBG blue-shift and recovery, as verified by the spectral

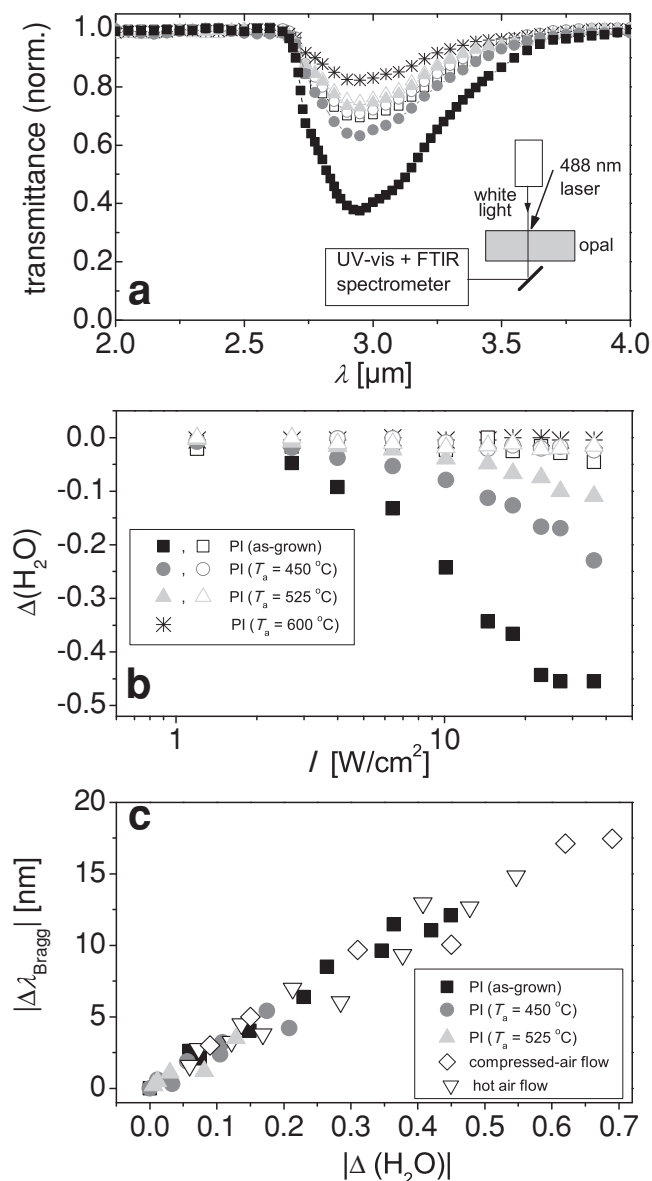


Figure 5. a) IR transmission spectra of infiltrated as-grown (black symbols) and annealed (at temperatures $T_a = 450$, 525, and 600 °C; gray, light gray, and star symbols, respectively) silica opals. The spectra were acquired before (solid symbols) and under photoirradiation (PI) with 488 nm light at $I = 20 \text{ mW cm}^{-2}$ (empty symbols). Experimental setup for in situ measurements of IR/UV-vis spectra during PI is shown as the inset. b) Amount of water desorbed from the opal during and after PI (solid and empty symbols, respectively). c) Correlation between the PGB shift, $|\Delta\lambda_{\text{Bragg}}|$, and the amount of desorbed water in the infiltrated opals induced by PI (solid symbols) and in bare opals or by air-drying (open symbols) – see legend. Data of the 600 °C-annealed opal under photoirradiation, which exhibited no change, are not shown. Photoexperiments were performed at $S = 0.002 \text{ mm}^2$.

changes. More-efficient desorption was obtained using hot air. The data obtained upon “drying” at different flow levels and temperatures, included in Figure 5c, show the same correlation as those achieved upon photoirradiation (note that the exact pressures and temperatures employed were irrelevant for this

experiment). In view of this, and regarding practical applications, varying ambient conditions like thermal fluctuations or airstreams have an obvious effect on the photonic properties of silica opals (and other water-containing PCs). A simple transparent sealing of a potential device should be enough to ensure reliable operability using this approach. On the other hand, an unshielded silica opal could be employed as a suitable sensor in some applications.

In conclusion, we have shown fast and reversible tunability of the pseudo bandgap in silica artificial opals by simple cw photoirradiation. We proposed dyeing the opal with a chromophore that absorbs in the UV-vis range to permit the use of inexpensive, low-intensity lasers as the light source. Photoabsorption of a focused 488 nm laser beam induced efficient local heating leading to fast water desorption and a subsequent bandgap shift, up to -12 nm , and response times of 20 ms. The effect was fully reversed as heat rapidly dissipated without active cooling, enabling high repeatability and fidelity in a fast fashion. The performance depended not only on the light intensity but also on the area of photoirradiation, so the photoexcitation of a reduced opal volume allowed fast temperature changes (heating and cooling). Thermal equilibrium with the non-irradiated structure limited the dynamic range and the maximum temperature achievable ($\approx 50 \text{ °C}$ in our setup). We explicitly demonstrated the univocal relationship between water removal from the opal and bandgap displacements. Thus, our approach also provides a simple optical means for the study of dynamic-water-sorption phenomena. The elucidation of the mechanisms governing the water desorption upon the prompt heating and, in particular, the fast rehydration of the opal requires further research, whereby the reported method could be a useful experimental tool. In summary, this simple and cost-effective method provides high, local switchability in conventional silica photonic crystals, offering an inexpensive solution for diverse applications.

Experimental Section

Fabrication of Opals: Artificial opals were prepared from dilute ethanol colloidal suspensions of monodisperse Stöber silica spheres (with diameter $D \approx 335 \text{ nm}$ and 3% polydispersity) by a vertical-deposition method on glass substrates under controlled temperature and humidity conditions.^[9] The resulting opals, formed by ≈ 20 spheres layers, were divided into several samples with an average size of $\approx 1000 \text{ mm}^2$. Some of the samples were annealed at 450, 525, or 600 °C over 5 hours in a conventional oven for controlled removal of silanol groups from the spheres surface.^[10,13]

Chromophore Infiltration: The opals were doped with an amino-thienyldioxycano-pyridine (ATOP-3), synthesized according to work by Würthner et al.^[18], $\approx 95\%$). Alternative chromophores were also used, obtaining similar results (not shown): methylene blue hydrate (Fluka, $\geq 95\%$) and protoporphyrin IX (Sigma, $\geq 95\%$). All of the chromophores exhibited significant absorption at the excitation wavelength (488 nm), and negligible photoluminescence, photoisomerization, or other non-linear optical effects under the conditions employed. The chromophore was dissolved in anhydrous, inhibitor-free tetrahydrofuran (THF) (Sigma-Aldrich) and the infiltration was accomplished by casting the solution onto the opal with a pipette. After rapid evaporation of the solvent, a portion of the neat chromophore remained on the sphere’s surface partially filling the opal voids. The dye could be simply removed by washing the opal with THF. The same absorbance (A) at 488 nm after infiltration, measured using a Cary Variant 4000 spectrometer, was

carefully pursued, so we adjusted the amount of chromophore to be dissolved in THF (amounts between 1.1 and 2.4 mg of dye were dissolved in 5 mL of THF) in each case. A was 0.26 in all of the samples.

Spectral Characterization: Visible-IR opal transmittance was measured by Fourier transform infrared spectrometry (IFS 66S Bruker) with a microscope attached. Physisorbed water largely contributed to the broad IR absorption band centered at $\approx 3 \mu\text{m}$ (around 3500 cm^{-1}) through O–H stretching of the hydrogen-bonded molecular water and SiO–H stretching of surface silanols bonded to molecular water.^[14] Bare and dye-infiltrated opals exhibited almost identical IR absorption bands, indicating that the chromophore deposition barely affected the water adsorption on the spheres. The amount of desorbed water ($\Delta(\text{H}_2\text{O})$, which is counted negative) was obtained from the decrease of the IR absorption band (integral from 2.6 to $3.3 \mu\text{m}$). This quantity was arbitrarily normalized to the IR integral of the as-grown opal. Dynamic changes of the opal PBC upon photoirradiation was characterized by reflectance spectroscopy performed on a small area ($\approx 20 \mu\text{m}^2$) using a fast diode array UV–vis spectrometer (Ocean Optics 2000+) with white light from a halogen lamp (Osram HLX 64623). To compare the response times of the rise and decay curves, we considered, respectively, the parameters τ_{rise} and τ_{decay} defined as the times needed to reach half of the stationary values. Transmittance in the near-UV region was measured by coupling an integrating sphere (Mikropack 50 mm) to the UV–vis spectrometer to minimize light scattering from the opal spheres.

Photonic Bandgap Properties: The Bragg peak position, at normal light incidence, is approximately given by $\lambda_{\text{Bragg}} = 2d_{111} \sqrt{fn_{\text{sphere}}^2 + (1-f)n_v^2}$, where f is the filling fraction of the opal and n_{sphere} and n_v the refractive indices of the spheres (silica) and the interstitial void region, respectively. n_v is the average (weighted) refractive index of the medium filling the voids (i.e., air, adsorbed water and, after infiltration, the chromophore). In the as-grown opals, λ_{Bragg} was 749 nm, while it shifted to 729, 712, and 699 nm after annealing at 450, 525, and 600 °C, respectively, mainly due to a d_{111} decrease resulting from the smaller amount of adsorbed water between spheres. After opal infiltration with the chromophore ($A = 0.26$), which led to an n_v increase, the resulting Bragg peaks were at 770, 749, 732, and 719 nm in the as-grown, 450, 525, and 600 °C-annealed opals, respectively. This redshift indicates a filling of $\approx 25\%$ of the void volume by the chromophore, according to calculations described by Gallego-Gómez et al.^[15]

Photoexcitation: Dye-infiltrated opals were illuminated with a 488 nm Ar⁺ laser line, while reflection spectra were simultaneously recorded. The acquisition time of the spectra was 2 ms, which is shorter than the response time of our system. The beam impinged with a small external incidence angle θ of 20 ° with respect to the normal of the opal, which prevented the reflected laser light from reaching the spectrometer. Back-scattered laser light was blocked using an edge filter placed before the spectrometer. An optical setup allowed the laser beam's full-width at half-maximum (FWHM) to be adjusted from 45 to 430 μm . The irradiated spot area was $S = \frac{\pi \text{FWHM}^2}{4 \cos \theta}$. The intensity ranged from 0.06 to 38 W cm^{-2} .

Acknowledgements

F.G.G. was supported by the JAE Postdoctoral Program from the CSIC. This work was partially funded by EU FP7 NoE Nanophotonics4Energy grant No. 248855; the Spanish MICINN CSD2007-0046 (Nanolight.es), MAT2009-07841 (GLUSFA), and the Comunidad de Madrid S2009/MAT-1756 (PHAMA) projects.

Received: July 12, 2012

Revised: August 14, 2012

Published online: September 14, 2012

- [1] J. F. Galisteo-López, M. Ibisate, R. Sapienza, L. S. Froufe-Pérez, A. Blanco, C. López, *Adv. Mater.* **2011**, *23*, 30.
- [2] M. Ozaki, Y. Shimoda, M. Kasano, K. Yoshino, *Adv. Mater.* **2002**, *14*, 514.
- [3] M. Kamenjicki, I. K. Lednev, S. A. Asher, *Adv. Funct. Mater.* **2005**, *15*, 1401.
- [4] A. C. Arsenault, D. P. Puzzo, I. Manners, G. A. Ozin, *Nat. Photon.* **2007**, *1*, 468.
- [5] J. R. Lawrence, G. H. Shim, M. G. Han, Y. Ying, P. Jiang, S. H. Foulger, *Adv. Mater.* **2005**, *17*, 2344.
- [6] K. Matsubara, M. Watanabe, Y. Takeoka, *Angew. Chem. Int. Ed.* **2007**, *46*, 1688.
- [7] J. Ge, Y. Yin, *Adv. Mater.* **2008**, *20*, 3485.
- [8] Y. Zhao, Z. Xie, H. Gu, C. Zhu, Z. Gu, *Chem. Soc. Rev.* **2012**, *41*, 3297.
- [9] F. Gallego-Gómez, A. Blanco, V. Canalejas-Tejero, C. López, *Small* **2011**, *7*, 1838.
- [10] F. Gallego-Gómez, A. Blanco, C. López, *J. Phys. Chem. C* **2012**, *116*, 18222.
- [11] H. Miguez, F. Meseguer, C. López, A. Mifsud, J. S. Moya, L. Vazquez, *Langmuir* **1997**, *13*, 6009.
- [12] M. D. Sacks, T.-Y. Tseng, *J. Am. Ceram. Soc.* **1984**, *67*, 526.
- [13] F. Gallego-Gómez, A. Blanco, D. Golmayo, C. López, *Langmuir* **2011**, *7*, 13992.
- [14] C. J. Brinker, G. W. Scherer, *Sol–Gel Science: The Physics and Chemistry of Sol–Gel Processing*, Academic, New York, **1990**, 581.
- [15] F. Gallego-Gómez, A. Blanco, D. Golmayo, C. López, *Adv. Funct. Mater.* **2011**, *21*, 4109.
- [16] L. T. Zhuravlev, *Colloids Surf. A* **1993**, *74*, 71.
- [17] J. N. Israelachvili, *Intermolecular and Surface Forces*, 2nd ed., Academic Press, London **1992**.
- [18] F. Würthner, S. Yao, J. Schilling, R. Wortmann, M. Redi-Abshiro, E. Mecher, F. Gallego-Gomez, K. Meerholz, *J. Am. Chem. Soc.* **2001**, *123*, 2810.